Available online at www.sciencedirect.com

ScienceDirect

Procedia Structural Integrity 2 (2016) 697–703

Structural Integrity Procedia

www.elsevier.com/locate/procedia

21st European Conference on Fracture, ECF21, 20-24 June 2016, Catania, Italy

Engineering Framework to Transfer the Lower Bound Fracture Toughness between Different Temperatures in the DBTT Region

Toshiyuki Meshii[a,*], Teruhiro Yamaguchi[b]

[a]*Faculty of Engineering, University of Fukui, 3-9-1 Bunkyo, Fukui-shi, Fukui, 910-8507, Japan*
[b]*Graduate Student, University of Fukui, 3-9-1 Bunkyo, Fukui-shi, Fukui, 910-8507, Japan*

Abstract

In this paper, an engineering framework to transfer the lower bound fracture toughness between different temperatures in the ductile–to–brittle (DBTT) temperature region is proposed and validated for 0.55% carbon steel using 0.5TSE(B) specimens. The framework requires only stress–strain curve for different temperatures as experimental data. The approach was based on the authors' finding that the critical stress σ_{22c} of the modified Ritchie–Knott–Rice criterion (the criterion predicts onset of cleavage fracture of a material in the DBTT transition temperature region, when the mid-plane crack-opening stress σ_{22} measured at a distance from the crack-tip equal to four times the crack-tip opening displacement δ_t, denoted as σ_{22d}, exceeds a critical value σ_{22c}) seems to be correlated with the lower bound fracture toughness for a specific specimen configuration. The proposed approach is expected to overcome some inconveniences which recent studies have reported to the Master Curve Local approaches to cleavage fracture that the Weibull parameters vary with size and temperature and are different from those stated in the Master Curve.

Peer-review under responsibility of the Scientific Committee of ECF21.

Keywords: lower bound toughness ; master curve ; modified Ritchie-Knott-Rice failure criterion ; temperature dependency

Nomenclature

B	Specimen thickness
B_o, B_x	Gross thickness of test specimens and of prediction

* Corresponding author. Tel.: +81-776-27-8468; fax: +81-776-27-9764.
E-mail address: meshii@u-fukui.ac.jp

Peer review under responsibility of the Scientific Committee of ECF21.
10.1016/j.prostr.2016.06.090

E	Young's modulus
J	J-integral
J_c, $J_{c\ FEA}$	Fracture toughness and J obtained at the fracture load P_c via FEA
J_s	J obtained at σ_{22d} converged
K_c	SIF corresponding to the fracture load P_c
K_{Jc}	An elastic-plastic equivalent SIF derived from the J-integral at the point of J_c
K_{Jcmed}	Median (50% cumulative failure probability) Master Curve fracture toughness
$K_{Jc(0.02)}$, $K_{Jc(0.98)}$	2 % lower bound and 98% upper bound of Master Curve fracture toughness
K_{max}	Maximum stress intensity factor during precracking
K_o	Scale parameter specified in ASTM E1921
M	$= (b_0\sigma_{YS})/J_c$: Parameter which gives information on the initial ligament size to fracture process zone size
N	Number of specimens tested
P	Load
P_c, P_Q	Fracture load and conditional value in ASTM E399
P_{max}, P_{min}	Maximum and Minimum force during precracking
P_s	P corresponding to J_s
V_g	Crack mouth opening displacement (CMOD)
W	Specimen width
a	Crack length of a test specimen
b_0	$= (W\text{-}a)$: Initial ligament length
δ_t	Crack-tip opening displacement (CTOD)
ν	Poisson's ratio
σ_B, σ_{B0}	True and nominal tensile strength
σ_{YS}, σ_{YS0}	True and nominal yield stress
σ_{22}	Crack-opening stress
σ_{22c}	Critical crack-opening stress
σ_{22d}	σ_{22} measured at a distance from the crack tip equal to four times δ_t at the specimen mid-plane
σ_{22d0}	Converged value of σ_{22d}

1. Introduction

Designing important components, such as reactor pressure vessels (RPVs), to operate at temperatures where the material behaves in a ductile manner is a conservative requirement intended to ensure that any crack, which may be present in the components, would extend in ductile manner. During operation RPV steel may be subject to neutron irradiation which reduces the ductile–to–brittle transition temperature (DBTT). Because continued operation of nuclear power plants thus requires that safety margin of RPV are demonstrated for operating temperature, temperature dependence of the fracture toughness of RPV steel has continuously collected attention of researchers and design engineers.

One of the widely accepted methods to predict the cleavage fracture toughness temperature dependence is the master curve approach (Wallin, 1993, 1998, 2002). The approach assumes the statistical weakest link model for cleavage fracture and uses Weibull distribution to express the scatter in fracture toughness K_{Jc}. The procedure is based on the concept of a normalized curve of "median" fracture toughness defined in terms of K_{Jc}-values for 1-T (25 mm thick) size specimens versus temperature applicable to hold experimentally for a wide range of ferritic pressure vessel and structural steels. Despite the efforts to apply the method, the approach is not without its limitations. For example, some recent studies have reported that the Weibull parameters vary with size and temperature and are different from those stated in the Master Curve, and thus, the K_{Jc} temperature dependence (Berejnoi and Perez Ipiña, 2015; James et al., 2014).

On the other hand, predicting the "lower bound" fracture toughness for a specific specimen configuration has been another interest. Chen et al. insisted that "it is necessary to distinguish the concepts of the lower bound toughness or the lower boundary of toughness values from that of the scatter band of toughness. The former is a

definite parameter determined by the specimen geometry and yielding properties, and the latter is statistical behaviour determined by the distribution of the weakest constituent (Chen et al., 1997).” We interpreted Chen’s opinion as that at least lower bound J_c for a specific specimen can be predicted by running an elastic–plastic finite element analysis (EP-FEA) with a given stress-strain relationship and a failure criterion. For this failure criterion, we considered ($4\delta_t$, σ_{22c}) criterion (Dodds et al., 1991),which predicts the onset of cleavage fracture when the crack-opening stress σ_{22}, measured at a distance from the crack tip equal to four times the crack-tip opening displacement (CTOD) δ_t, hereinafter denoted as σ_{22d}, exceeds a critical value σ_{22c}. This criterion was validated to explain the crack depth dependence on J_c (Dodds et al., 1991) and to explain the test specimen thickness effect on J_c (Lu and Meshii, 2014a, b, 2015; Meshii et al., 2015; Meshii et al., 2013; Meshii and Tanaka, 2010; Meshii et al., 2010). Through examination of the applicability of the ($4\delta_t$, σ_{22c}) criterion to the decommissioned RPV steel J_c database ranged with specimen thicknesses 8 to 254 mm (Meshii and Yamaguchi, 2016), we reached an idea (Fig. 1 left) that the convergence of σ_{22d} for increasing load is necessary for fracture initiation, because critical value σ_{22c} is equal to the converged value of σ_{22d}. Considering the fact fracture always occurred after σ_{22d} reached σ_{22c}, it seemed that it seems that the minimum J that satisfy $\sigma_{22d} = \sigma_{22c}$ corresponds to the lower bound fracture toughness observed for the specimen and the material considered. It was also considered that the existence of the lower bound J is consistent with Chen et al.’s opinion (Chen et al., 1997).

Under this observation, it was considered that temperature dependency of J_c might be predicted from the convergence of σ_{22d} calculated by EP-FEA, with tensile test data for the corresponding temperature.

In this study, large-strain EP-FEA were conducted for 0.55 % carbon steel with tensile test data for two temperatures, i.e., 20 and -25 °C, to predict the lower bound value of J_c (hereinafter denoted as J_s) for each temperature by the proposed engineering framework. By comparing the predicted values with the experimental results, the validity of the proposed framework was confirmed.

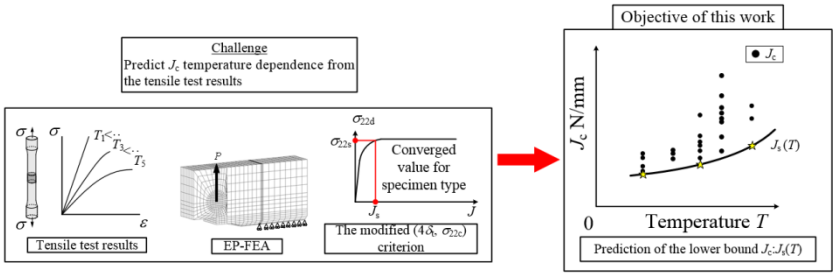

Fig. 1 Engineering framework to predict the temperature dependence of the lower bound J_c for a specimen

2. Engineering framework to predict the temperature dependence of the lower bound J_c

The proposed method to predict the temperature dependency of the lower bound J_c is as follows.

a. Determine the DBTT region, lower shelf temperature T_L and upper shelf temperature T_U from the Charpy impact test result.
b. Conduct tensile tests at multiple temperatures T_i (i ; at least 2) within T_L and T_U and obtain the relationship between true-stress and true-strain for the temperature T_i.
c. Conduct EP-FEA for each temperature and calculate the relationship between J and σ_{22d} for each load step. Here, in EP-FEA, the crack length a and the specimen width W ratio $a/W = 0.50$ was used.
d. For each temperature T_i, determine predicted lower bound fracture toughness J_{si} as J corresponding to converged σ_{22d}.

3. Material selection

Considering nominal tensile strength σ_{B0} and nominal yield stress σ_{YS0} ratio σ_{B0}/σ_{YS0} for EURO RPVs and Japanese RPVs is equal to 1.3, 0.55% carbon steel JIS S55C, which is known to be in the transition temperature region at around room temperature and has larger σ_{B0}/σ_{YS0}, is selected for examination.

The chemical contents of S55C were C: 0.55 %, Si: 0.17 %, Mn: 0.61 %, P: 0.015 %, S: 0.004 %, Cu: 0.13 %, Ni: 0.07 % and Cr: 0.08 %, respectively. The material was quenched at 850 °C and tempered at 650 °C.

Charpy impact test results and true stress true strain curve obtained from tensile test are shown in Fig. 2. From Charpy impact test result, -25 and 20 °C were selected as the test temperature. As results of the tensile test at -25 ºC, Young's modulus E, σ_{YS0} and σ_{B0} of 214 GPa, 481 MPa and 778 MPa were obtained, respectively. For 20 °C, E, σ_{YS0} and σ_{B0} of 206 GPa, 394 MPa and 710 MPa were obtained, respectively. True stress – true strain curves used in the EP-FEA are shown in Fig. 3. Poisson's ratio ν of 0.3 was used in the analysis for both temperatures.

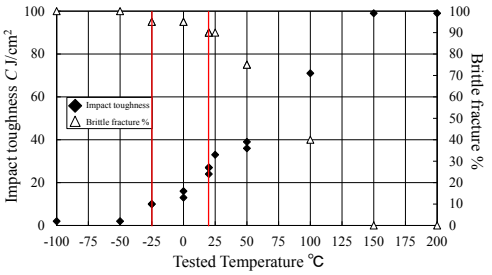

Fig. 2 Charpy impact test result of S55C

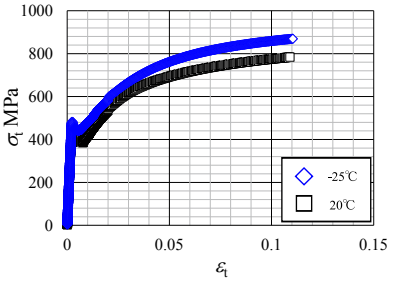

Fig. 3 True stress–true strain curve of S55C

4. EP-FEA

The dimensions of SE(B) specimen are shown in Fig. 4. Considering symmetry conditions, one quarter of an SE(B) specimen containing a straight crack was analyzed, with appropriate constraints imposed on the symmetry planes, as illustrated in Fig. 5. An initial blunted notch of radius ρ was inserted at the crack tip. In this study, the FEA models were generated by referring the FEA model of Gao et al.'s paper (Gao and Dodds, 2000). For all cases, 20-noded isoparametric three-dimensional (3-D) solid elements with reduced (2 × 2 × 2) Gauss integration were employed. The material behavior in the FEA was assumed to be governed by the J2 incremental theory of plasticity, the isotropic hardening rule, and the Prandtl–Reuss flow rule. The piecewise linear total true stress–strain curve of the S55C steel shown in Fig. 3 was used in the EP-FEA. The load–line displacement was applied for each EP-FEA. In the EP-FEA, the applied load P was measured as the total reaction force on the supported nodes. The J simulated by the EP-FEA, denoted by J_{FEA}, was evaluated using a load-vs.-crack-mouth opening displacement diagram (P–V_g diagram), accordance with ASTM E1921 (ASTM, 2010). WARP3D (Gullerud et al., 2014) was used as the FEA solver.

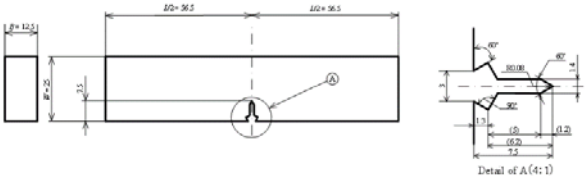

Fig. 4 Dimensions of SE(B) specimen

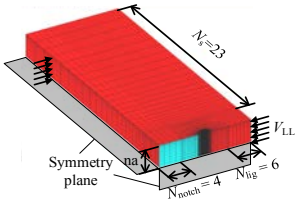

Fig. 5 FEA model for SE(B) specimen

5. Prediction of the lower bound J_c at the two temperatures as J_s

After confirming that the linear portion of the EP-FEA P-V_g diagrams showed good agreement with the relationship described in the ASTM E1820 (ASTM, 2006), the relationships between σ_{22d}: σ_{22} measured at a distance from the crack tip equal to $4\delta_t$ at the specimen mid-plane and J_{FEA} calculated from P–V_g diagram for each load step were summarized in Fig. 6.

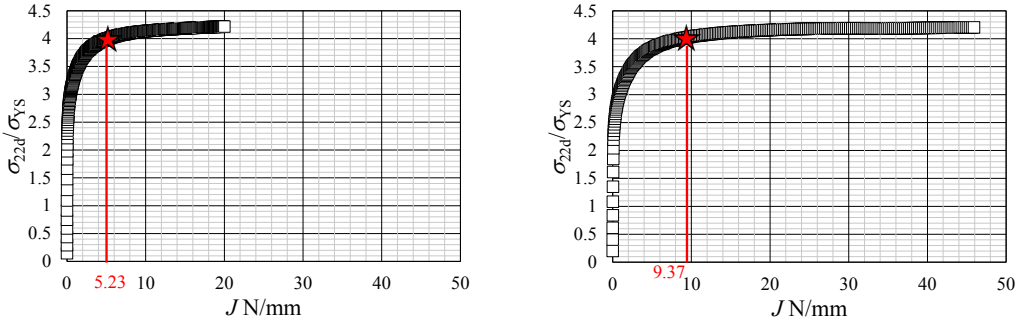

(a) (-25 °C) (b) (20 °C)

Fig. 6 σ_{22d}/σ_{YS}-J diagram; star mark represent the predicted lower bound J_c, denoted as J_s

For both temperatures, σ_{22d} showed converging tendency for increasing J_{FEA}, as expected from our experience with SE(B) specimens in the range of 8–254 mm thickness and RPV material (Meshii and Yamaguchi, 2016). Considering the fact that fracture always occurred after σ_{22d} reached σ_{22c}, and Chen's opinion that the minimum J_c can be predicted by EP-FEA, we expected that J_{FEA} corresponding to $\sigma_{22d} = \sigma_{22c}$, hereinafter denoted as J_S, gives an engineering prediction of the lower bound J_c for the specific specimen at specified temperature. Since there is not a definite method to determine the converged value of σ_{22d}, i.e., σ_{22s}, here we applied the method described below. First, an i-th σ_{22d} is defined as σ_{22di} and σ_{22d} which obviously converged is defined as σ_{22d0}. Then, a norm S_n was defined as below

$$S_n = \{\sum_{i=1}^{n} (\sigma_{22di} - \sigma_{22d0})^2\}^{1/2} \tag{1}$$

and J at the value of S_n/S_{n+1} is equal to 0.9999 was defined as J_s: the predicted lower bound fracture toughness. By using this method, the values of J_s were predicted as 5.23 N/mm for -25 °C and 9.37 N/mm for 20 °C as shown in Table 1. K_{Js} in the Table is the J_s in the term of stress intensity factor, calculated as $\{J_sE/(1-\nu^2)\}^{1/2}$, using Young's modulus E at respective temperature and Poisson's ratio $\nu = 0.3$. P_s is the load corresponding to J_s.

Table 1 The predicted J_s for each test temperature

T (°C)	σ_{22d0} (MPa)	J_s (N/mm)	K_{Js} (MPam$^{1/2}$)	P_s (kN)
-25	1804	5.23	35.1	6.15
20	1656	9.37	46.1	7.74

The tendency that J_s is increasing with increasing of the test temperature, which often appeared in the past experiences, was obtained.

6. Fracture toughness test

Fracture toughness test was conducted in accordance with ASTM E1921 (ASTM, 2010). The dimensions of SE(B) specimen are shown in Fig. 4.

Fatigue precrack was inserted with loads corresponding to K_{max} = 22 and 19 MPam$^{1/2}$ for the 1st and last stages, respectively, which satisfied the requirement of the ASTM E1921 requiring K_{max} to be ≤ 25 and 20 MPam$^{1/2}$, respectively. The reduction in P_{max} these load steps was 18.7 %, which satisfied the requirement to be not greater than 20 %. The load ratio $R = P_{min}/P_{max}$ was applied, and the load frequency was 10 Hz.

In fracture toughness test, the loading rate was controlled to be 1.2 MPam$^{1/2}$/s, which is in the specified range of 0.1–2.0 MPam$^{1/2}$/s. The test specimen temperature was maintained to be in the range of 20 ± 1 °C and -25 ± 1 °C for 30 minutes, which satisfied ASTM requirement of T ± 3 °C and 15 minutes.

Six test results for 20 °C and -25 °C, which satisfied ASTM E1921 requirements, were summarized in Table 2. Here, in Table 2, μ and Σ denotes the median and standard deviation of each value, respectively. $2\Sigma/\mu$ % is a

reference value intended to represent the magnitude of data scatter. Considering that the predicted scatter of K_{Jc} in the standard as $2\Sigma/\mu = 56\ (1\text{-}20/\mu)$ % was 38.5 and 46.3 % for -25 and 20 °C, respectively, the observed scatter was considered as within the expected range in an engineering sense.

Table 2 Fracture toughness test results for S55C (SE(B), W = 25 mm, B/W = 0.5)

T (°C)	Specimen ID	1	2	3	4	5	6	μ	Σ	$2\Sigma/\mu$ (%)
-25	a/W	0.50	0.50	0.50	0.50	0.50	0.50			
	P_c (kN)	9.71	10.4	9.86	8.98	10.2	10.2			
	K_c (MPam$^{1/2}$)	51.8	55.4	53.8	47.8	54.9	54.7			
	J_c (N/mm)	15.5	19.6	19.9	12.5	19.0	18.6			
	K_{Jc} (MPam$^{1/2}$)	60.4	67.9	68.4	54.2	66.8	66.1	64.0	5.58	17.4
	M	345	273	269	428	282	288			
20	a/W	0.50	0.50	0.50	0.50	0.50	0.50			
	P_c (kN)	10.5	11.4	10.6	10.8	11.9	12.6			
	K_c (MPam$^{1/2}$)	56.4	61.8	56.8	57.4	65.0	67.9			
	J_c (N/mm)	30.5	67.7	39.6	41.1	96.3	98.1			
	K_{Jc} (MPam$^{1/2}$)	83.1	124	94.7	96.5	148	149	116	28.6	49.3
	M	161	72.7	124	120	51.1	50.2			

The path of the P-V_g diagrams obtained from experiments and EP-FEA are similar for each temperature, and thus reproducibility of the data was confirmed. Fracture load P_c to the conditional value P_Q ratio P_c/P_Q was larger than 1.1 for all P_cs, and thus these fracture toughness test results were considered as valid for K_{Jc} tests. It was also confirmed that predicted minimum fracture load P_s for each temperature is smaller than the experimentally obtained P_cs. The difference between P_s and the smallest P_c for -25 and 20 °C were 46.0 and 35.7 %, respectively.

Master curve reference temperature T_0 was obtained as 30.6 °C from the test results of -25ºC, and master curve for 1T specimen K_{Jc1T} was obtained as follows.

$$K_{Jc1T} = 30 + 70\exp\left[0.019(T - 30.6)\right] \tag{2}$$

Because the specimen under consideration is of 12.5 mm thickness, the estimated master curve for this thickness $K_{Jc0.5T}$ was described as follows.

$$K_{Jc0.5T} = 20 + \{K_{Jc1T} - 20\}(25/12.5)^{1/4} \tag{3}$$

This master curve together with 2% and 98% tolerance bound curves for T_0 = 30.6 °C described as follows was compared with the experimental results in Fig. 7. The predicted lower bound of K_{Js} is also shown in Fig. 7. Note that the master curves in Fig. 7 are for 0.5T thickness, using Eq. (3).

$$K_{Jc0.5T(0.02)} = 20 + \{0.415K_{Jc1T} + 11.70 - 20\}(25/12.5)^{1/4} \tag{4}$$

$$K_{Jc0.5T(0.98)} = 20 + \{1.547K_{Jc1T} - 10.94 - 20\}(25/12.5)^{1/4} \tag{5}$$

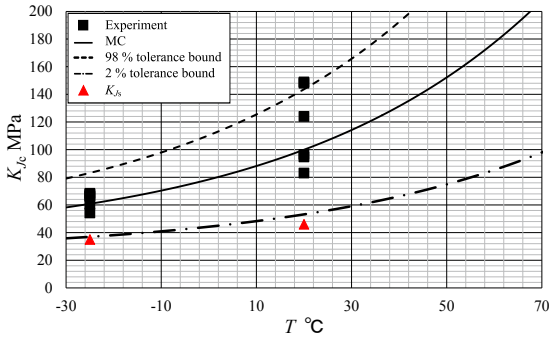

Fig. 7 Comparison of the predicted K_{Js} with the experimental values and the master curve 2% tolerance bound

From Fig. 7, it is read that the predicted K_{Js}s were conservative compared with the experimental results and even with the master curve 2 % tolerance bound. Though there might be an opinion that 2% tolerance bound is still not a lower bound K_{Jc} in a strict sense, K_{Js} seemed to give a good estimate of the lower bound K_{Jc} in an engineering sense. Thus, it was concluded that J_s obtained from the proposed framework has a possibility to predict the temperature dependence of lower bound fracture toughness in an engineering sense.

7. Conclusion

In this paper, an engineering framework to predict the temperature dependence of the lower bound fracture toughness for a specified specimen in an engineering sense was proposed. The framework has an advantage on the point it requires only stress-strain curve as experimental data. The framework was validated by showing that the predicted K_{Js} for a specified temperature were fairly smaller than the experimental results, and that these K_{Js} were slightly smaller than the 2% tolerance bound K_{Jc}, predicted by the master curve method.

References

ASTM, 2006. E1820-06a Standard Test Method for Measurement of Fracture Toughness, Annual Book of ASTM Standards. American Society for Testing and Materials, Philadelphia PA.

ASTM, 2010. E1921-10 Standard Test Method for Determination of Reference Temperature, T_o, for Ferritic Steels in the Transition Range, Annual Book of ASTM Standards. American Society for Testing and Materials, Philadelphia PA.

Berejnoi, C., Perez Ipiña, J.E., 2015. Analysis of Size and Temperature Effects in the Ductile to Brittle Transition Region of Ferritic Steels. Engineering Fracture Mechanics 148, 180–191.

Chen, J.H., Wang, G.Z., Yan, C., Ma, H., Zhu, L., 1997. Advances in the Mechanism of Cleavage Fracture of Low Alloy Steel at Low Temperature. Part II: Fracture Model. International Journal of Fracture 83, 121−138.

Dodds, R.H., Anderson, T.L., Kirk, M.T., 1991. A Framework to Correlate a/W Ratio Effects on Elastic-Plastic Fracture Toughness (J_c). International Journal of Fracture. 48, 1–22.

Gao, X., Dodds, R.H., 2000. Constraint Effects on the Ductile-to-Brittle Transition Temperature of Ferritic Steels: A Weibull Stress Model. International Journal of Fracture 102, 43–69.

Gullerud, A., Healy, B., Koppenhoefer, K., Roy, A., RoyChowdhury, S., Petti, J., Walters, M., Bichon, B., Kristine, C., Carlyle, A., Sobotka, J., Mark, M., Dodds, R.H., 2014. WARP3D Release 17.5.3 Manual. University of Illinois at Urbana-Champaign.

James, P.M., Ford, M., Jivkov, A.P., 2014. A Novel Particle Failure Criterion for Cleavage Fracture Modelling Allowing Measured Brittle Particle Distributions. Engineering Fracture Mechanics 121–122, 98–115.

Lu, K., Meshii, T., 2014a. Application of T_{33}-stress to Predict the Lower Bound Fracture Toughness for Increasing the Test Specimen Thickness in the Transition Temperature Region. Advances in Materials Science and Engineering 2014, 1–8, DOI://10.1155/2014/269137

Lu, K., Meshii, T., 2014b. Three-Dimensional T-stresses for Three-Point-Bend Specimens with Large Thickness Variation. Engineering Fracture Mechanics 116, 197–203.

Lu, K., Meshii, T., 2015. A Systematic Investigation of T-stresses for a Variety of Center-Cracked Tension Specimens. Theoretical and Applied Fracture Mechanics 77, 74–81.

Meshii, T., Lu, K., Fujiwara, Y., 2015. Extended Investigation of the Test Specimen Thickness (TST) Effect on the Fracture Toughness (J_c) of a Material in the Ductile-to-Brittle Transition Temperature Region as a Difference in the Crack Tip Constraint—What Is the Loss of Constraint in the TST Effects on J_c? Engineering Fracture Mechanics 135, 286–294.

Meshii, T., Lu, K., Takamura, R., 2013. A Failure Criterion to Explain the Test Specimen Thickness Effect on Fracture Toughness in the Transition Temperature Region. Engineering Fracture Mechanics 104, 184–197.

Meshii, T., Tanaka, T., 2010. Experimental T_{33}-stress Formulation of Test Specimen Thickness Effect on Fracture Toughness in the Transition Temperature Region. Engineering Fracture Mechanics 77, 867−877.

Meshii, T., Tanaka, T., Lu, K., 2010. T-stress Solutions for a Semi-Elliptical Axial Surface Crack in a Cylinder Subjected to Mode-I Non-Uniform Stress Distributions. Engineering Fracture Mechanics 77, 2467–2478.

Meshii, T., Yamaguchi, T., 2016. Applicability of the Modified Ritchie–Knott–Rice Failure Criterion to Transfer Fracture Toughness J_c of Reactor Pressure Vessel Steel Using Specimens of Different Thicknesses—Possibility of Deterministic Approach to Transfer the Minimum J_c for Specified Specimen Thicknesses. Theoretical and Applied Fracture Mechanics, in press, http://dx.doi.org/10.1016/j.tafmec.2016.04.002

Wallin, K., 1993. Irradiation Damage Effects on the Fracture Toughness Transition Curve Shape for Reactor Pressure Vessel Steels. International Journal of Pressure Vessels and Piping 55, 61−79.

Wallin, K., 1998. Master Curve Analysis of Ductile to Brittle Transition Region Fracture Toughness Round Robin Data. The “Euro” Fracture Toughness Curve. VTT Publications 367.

Wallin, K., 2002. Master Curve Analysis of the “Euro” Fracture Toughness Dataset. Engineering Fracture Mechanics 69, 451–481.